Oxidation Phenomena in Advanced High Strength Steel – ZCO-62

Oxidation, wetting and work of adhesion of 1.8 Mn and 1.9 Mn + 1.0 Si alloyed steels

Yuliu You, Junki Kim, Wim G. Sloof

Delft University of Technology
Department of Materials Science and Engineering
Surface and Interface Engineering

Objective

Study the effect of surface oxides due to selective oxidation during annealing of AHSS at various dew points on the wetting and work of adhesion

Increasing the dewpoint of the annealing atmosphere promotes internal oxidation rather than external oxidation

Surface oxides generally reduces the wetting and work of adhesion

Content

- Internal versus external oxidation
- Oxides at coating interface after hot-dip galvanizing
- Annealing experiments
- Dewetting experiments
- Contact angle and work of adhesion
- Summary & future work

1.

Internal versus external oxidation

External versus internal oxidation

Example Fe-Mn binary alloy

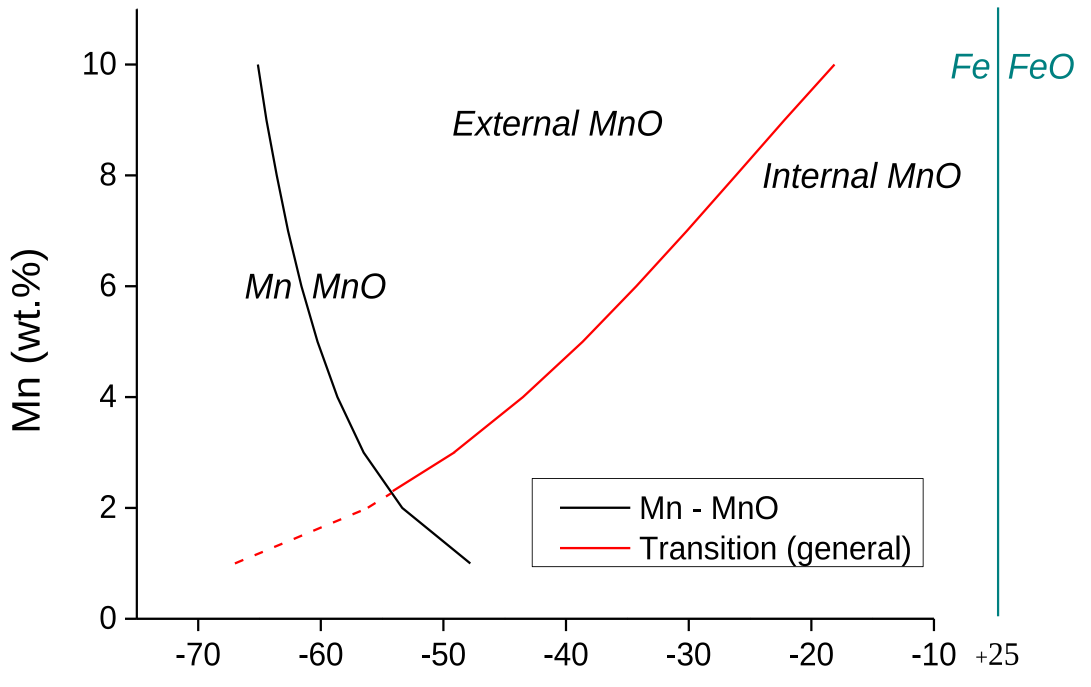

5 vol.% H_2 in H_2+N_2 mixture

V.A. Lashgari, C. Kwakernaak, W.G. Sloof, Transition from Internal to External Oxidation of Mn Steel Alloys, Oxid Met (2014) 435-451

External versus internal oxidation

Example Fe-Mn binary alloy

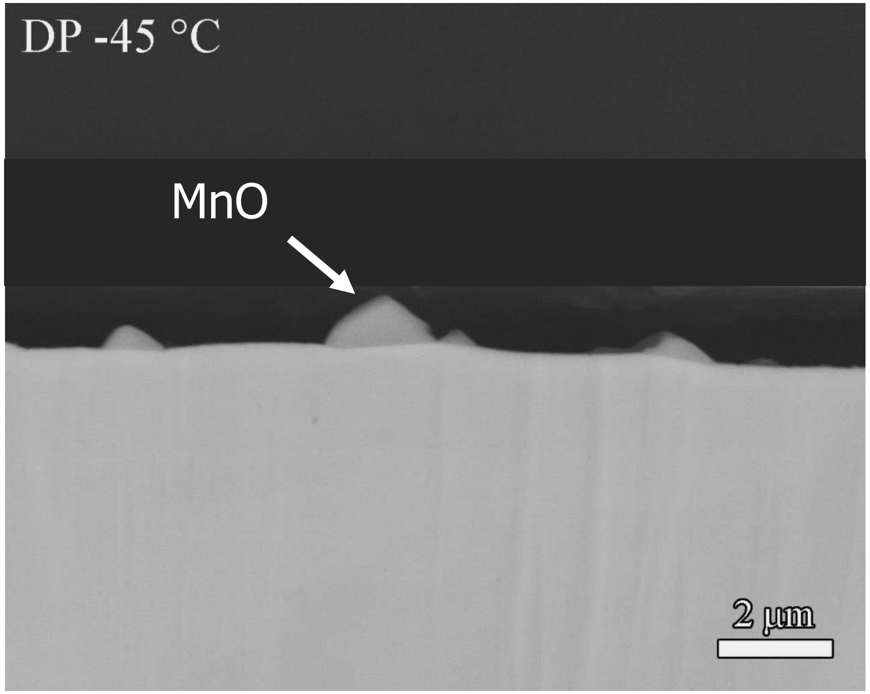

external oxidation

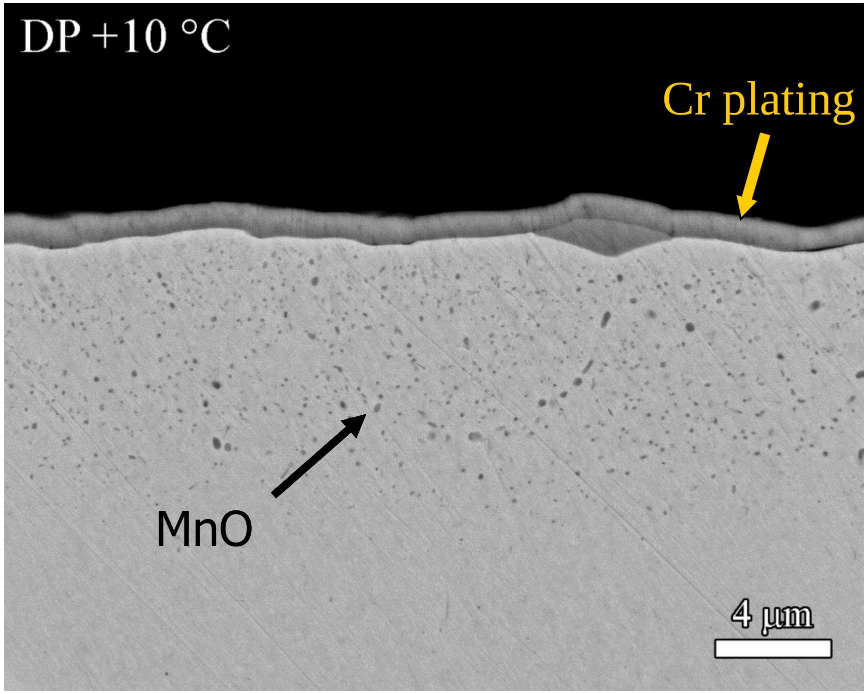

internal oxidation

Increasing annealing dew point promotes internal oxidation

V.A. Lashgari, C. Kwakernaak, W.G. Sloof, Transition from Internal to External Oxidation of Mn Steel Alloys, Oxid Met (2014) 435-451

External versus internal oxidation

Annealing in 5 vol.% H_2 in $H_2 + N_2$ mixture @ 850 °C

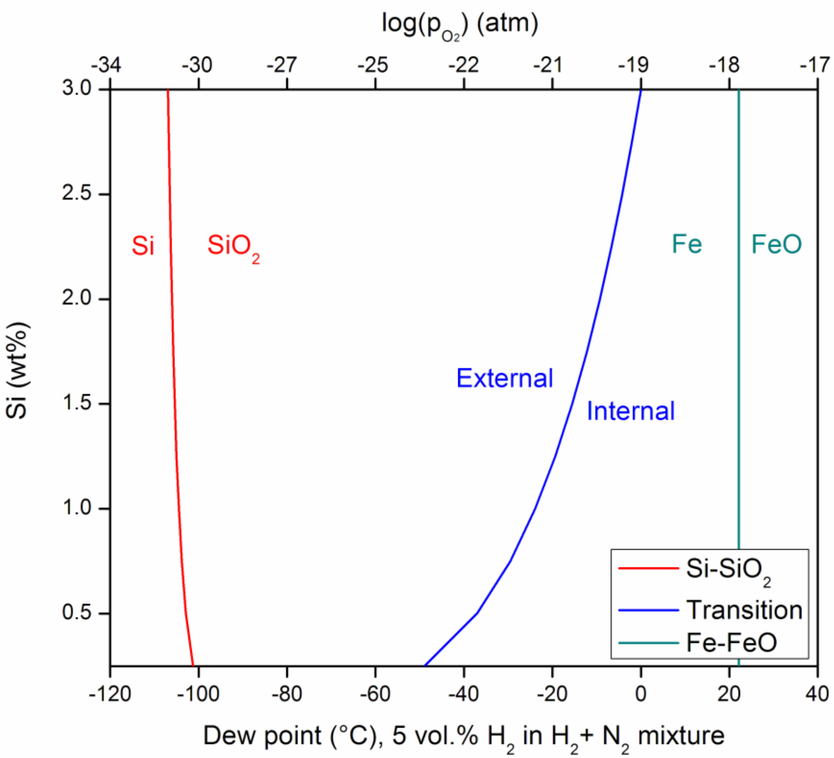

Binary Fe- Si

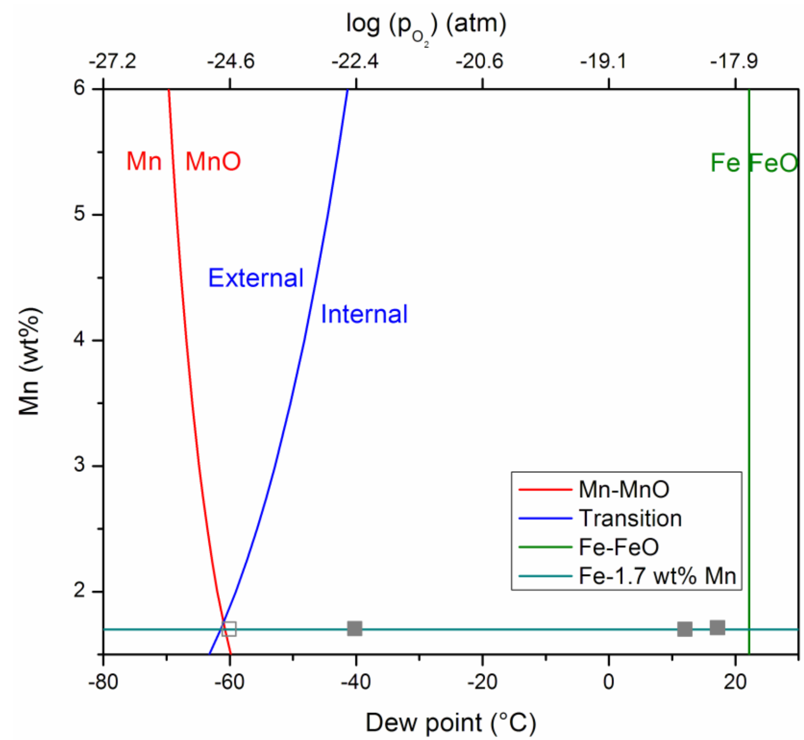

Binary Fe- Mn

Modification of Wagner's criterion

- Grain boundaries

$$N^{(0)}_{B,critical\ (GB)} = \left[\frac{\pi g^* V_{alloy} N_O^{(s)} D_O^{(GB)}}{2\upsilon V_{BO_\upsilon} D_B^{(GB)}} \right]^{1/2}$$

$$D_i^{(GB)} = D_i^{(0)} \exp\left(-Q_i / 2RT\right)$$

- Multi-component alloy

$$\left[\sum_B N_B^{(0)} \left[\upsilon D_B V_{BO_\upsilon} \right]^{1/2} \right] \geq \left[\frac{\pi g^* V_{alloy} N_O^{(s)} D_O}{2} \right]^{1/2}$$

Effect of Si addition on transition dew point of Fe-1.8 wt% Mn alloy

Alloying element	1 wt% Si	1.8 wt% Mn	1.8 wt% Mn 1 wt% Si
Transition DP (^{0}C)	-38	-59	-34

Annealing Mn + Si steels

Low oxygen potential – External oxidation
High oxygen potential – Internal Oxidation

Si/Mn ratio:
high mainly SiO_2
low mainly Mn_2SiO_4

$$Si + O_2 = SiO_2$$

$$2SiO_2 + 2Mn + O_2 = 2MnSiO_3$$

$$2MnSiO_3 + 2Mn + O_2 = 2Mn_2SiO_4$$

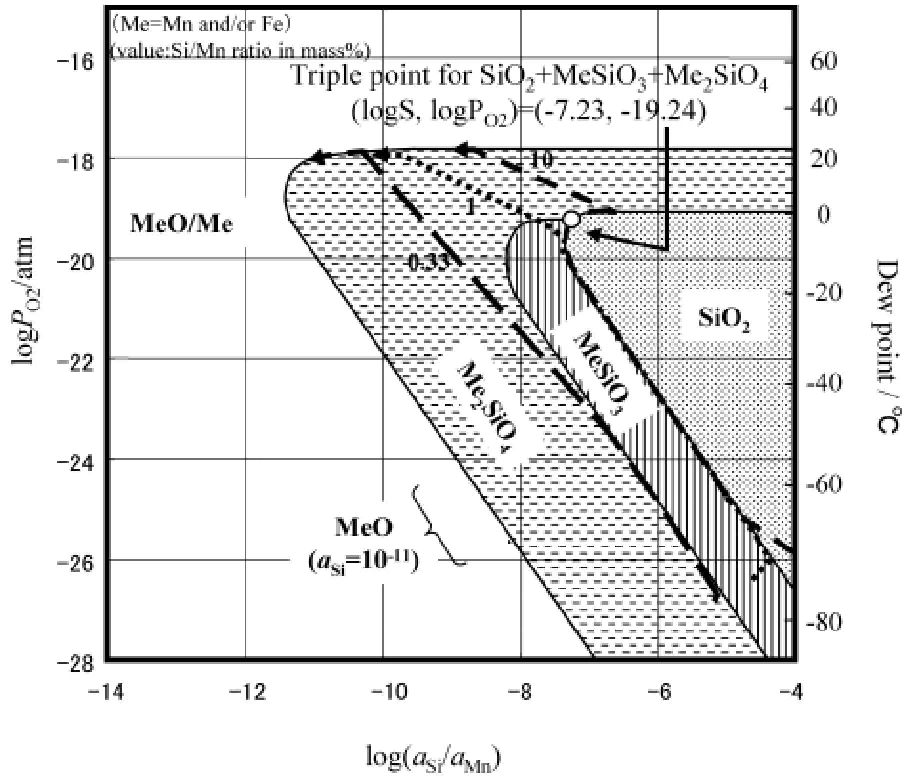

Chemical potential diagram of Fe–Si–Mn–O system at 850°C, Annealing in 5 vol.% H_2 in H_2 + N_2 mixture, calculated with FactSage - Suzuki et. al., ISIJ International, Vol. 49, No. 4 (2009) 564-573

Surface oxides

Fe-Mn binary steel

Sample composition (wt%):

C	Mn	Si	Al
0.103	1.7	0.049	0.002

Surface oxide is mainly MnO

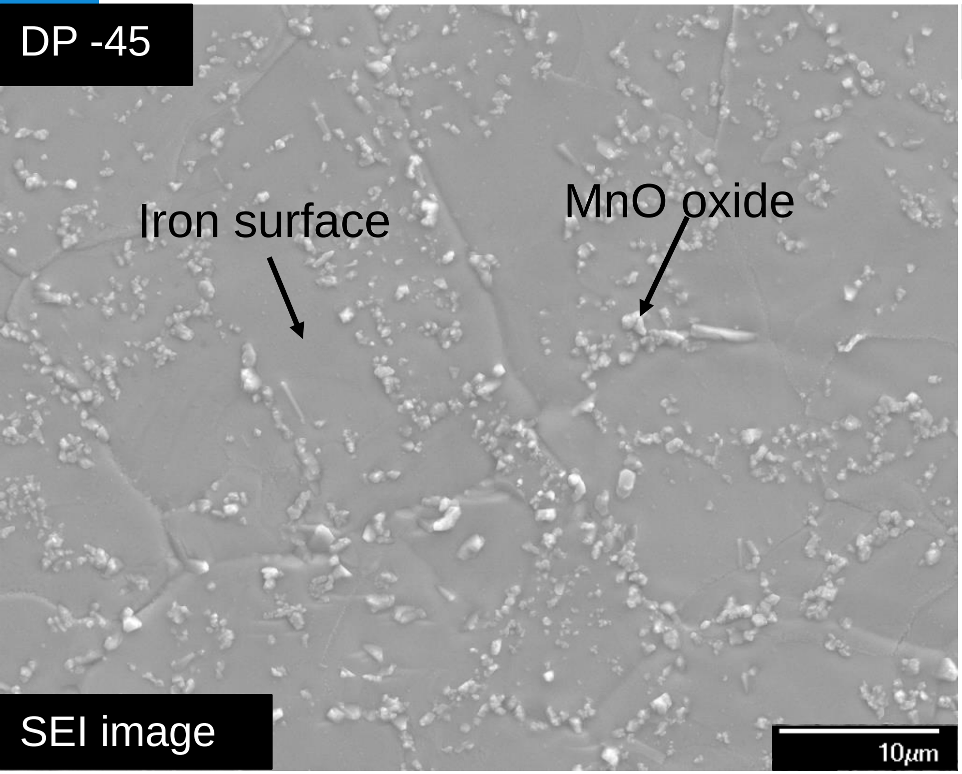

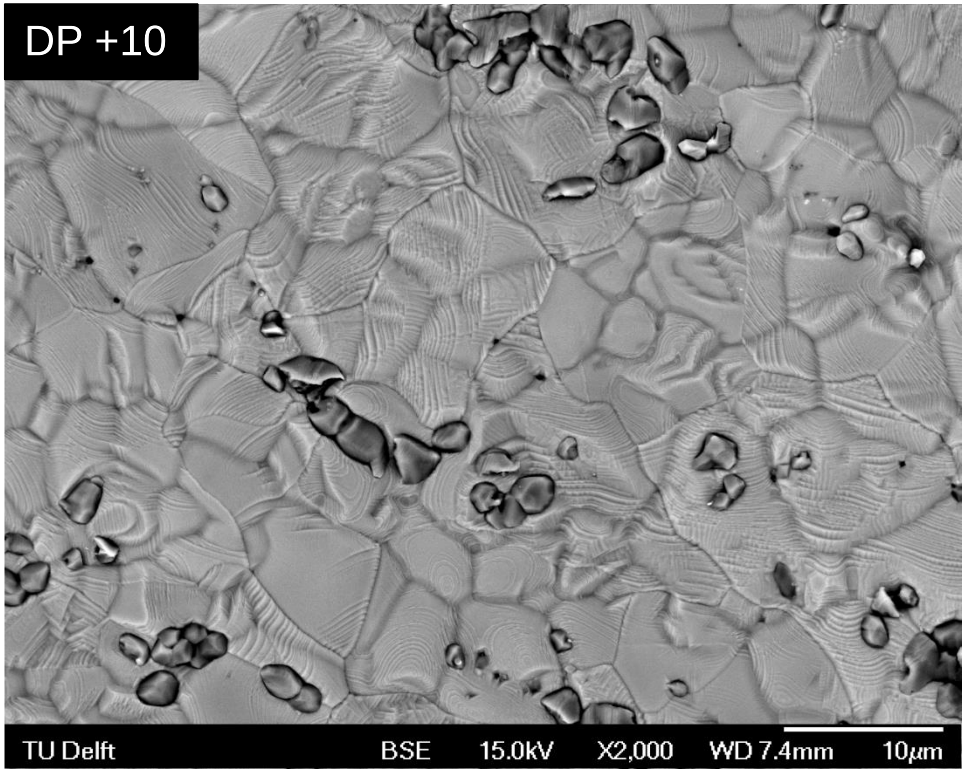

Size of surface oxides increases at high dew point

Surface oxides

Fe-Mn-Si

Steel composition (wt%):

C	Mn	Si	Al
0.104	1.9	0.94	0.017

Surface oxide is mainly Mn_2SiO_4

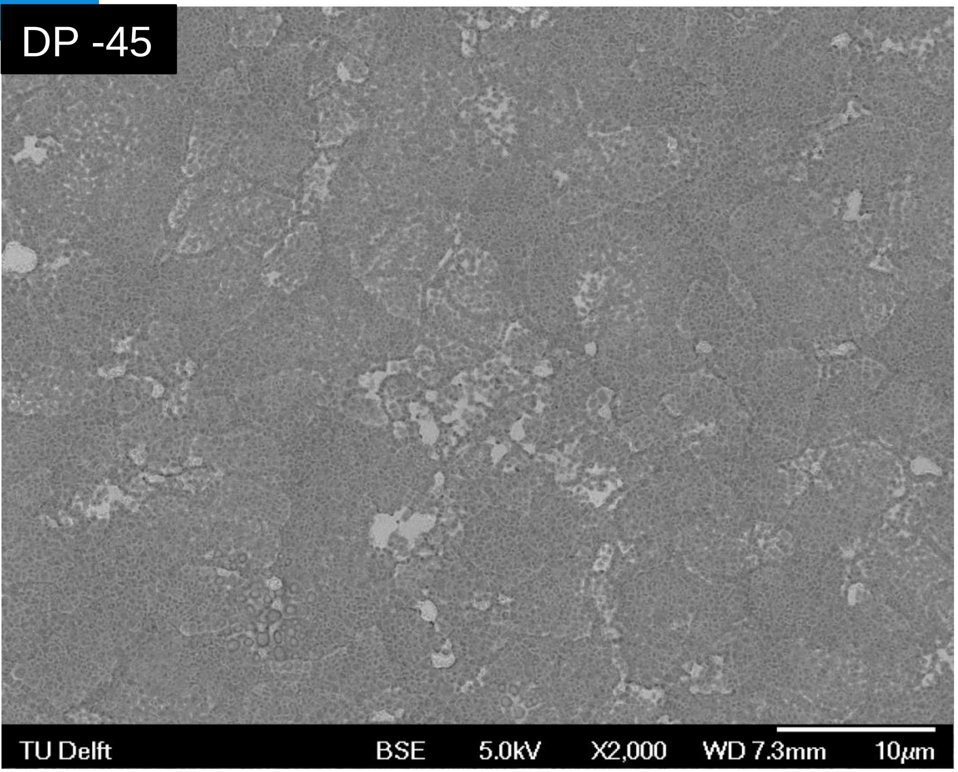

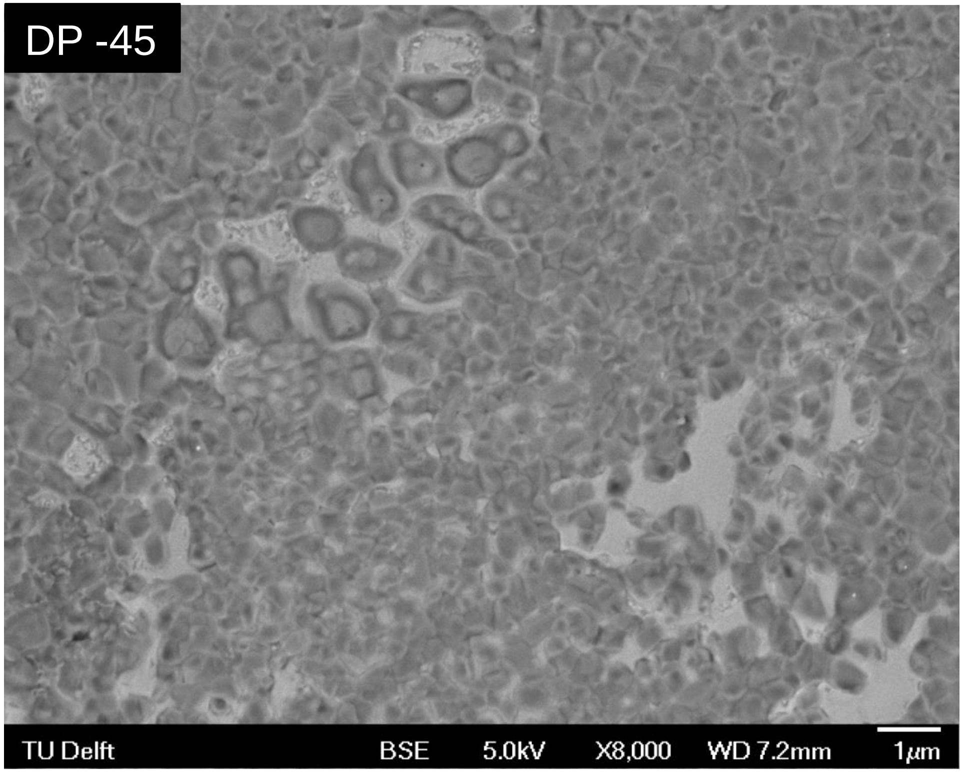

Si enhances formation of external oxides significantly

Surface oxides

Fe-Mn-Si

Steel composition (wt%):

C	Mn	Si	Al
0.104	1.9	0.94	0.017

Surface oxide is mainly Mn_2SiO_4

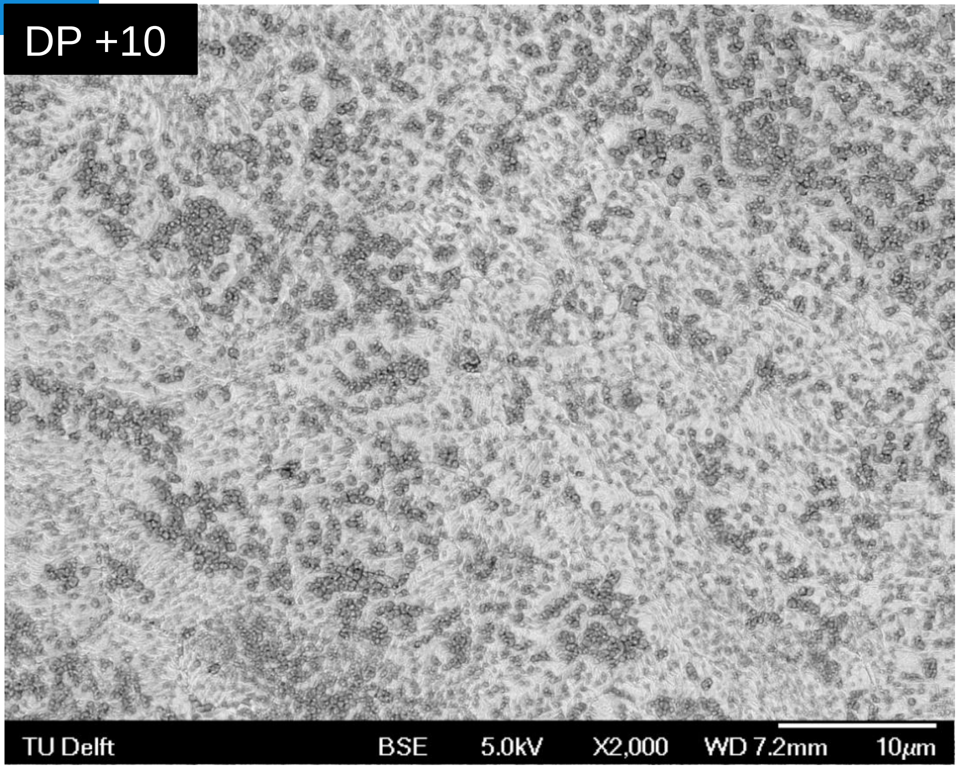

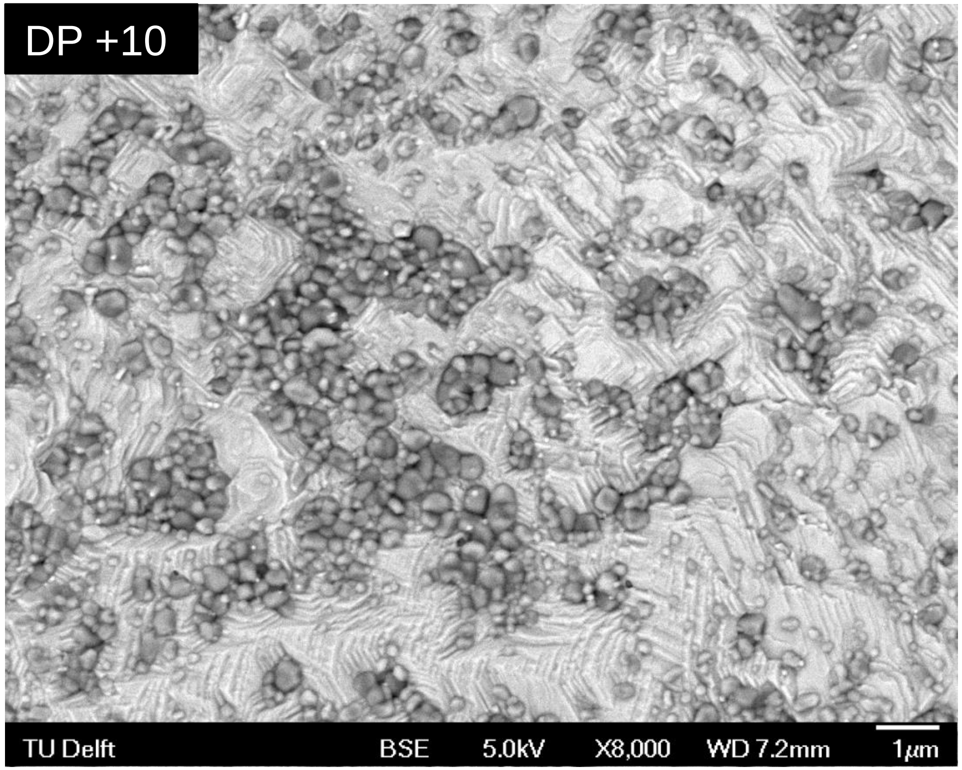

Formation of external oxides is suppressed with increasing dew point

SEM cross-section observation

Fe-Mn-Si

Steel composition (wt%):

C	Mn	Si	Al
0.104	1.9	0.94	0.017

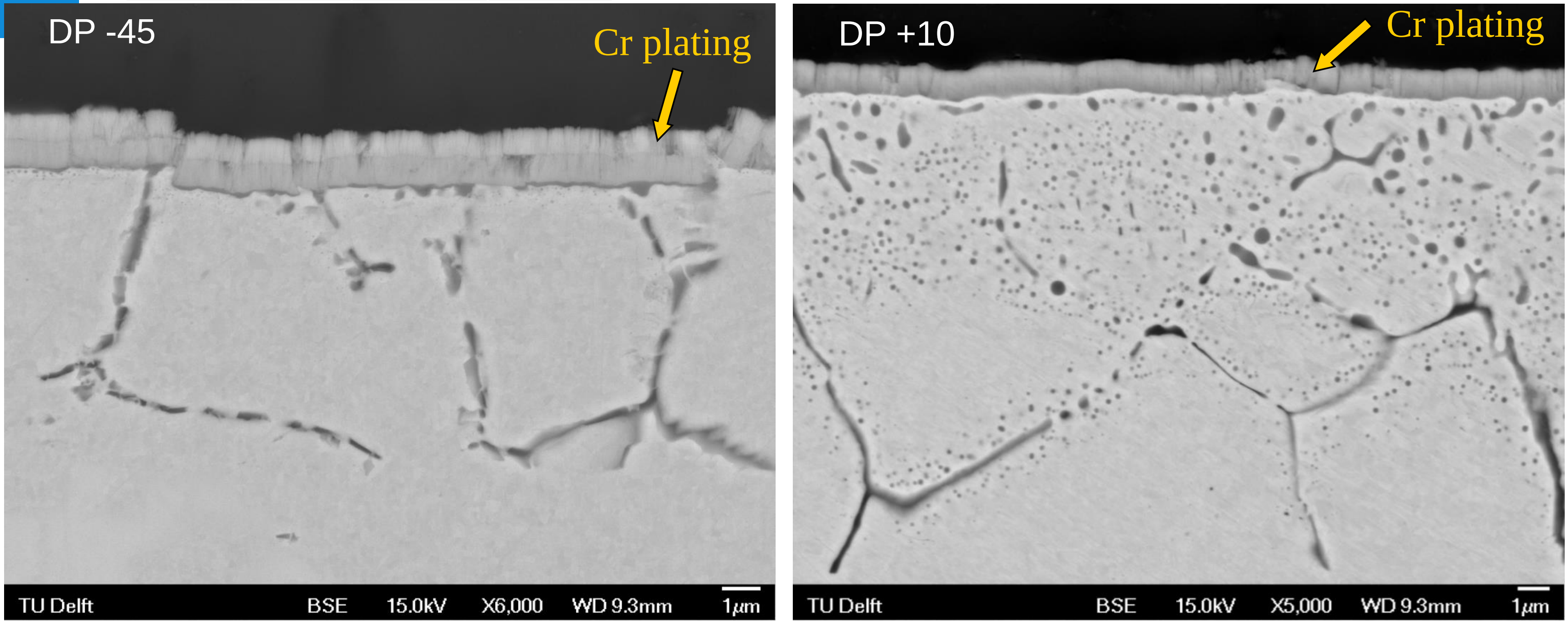

Si promotes Mn_2SiO_4 formation along grain boundaries

2.

Oxides at coating interface after hot-dip galvanizing

Surface oxides and coating adhesion

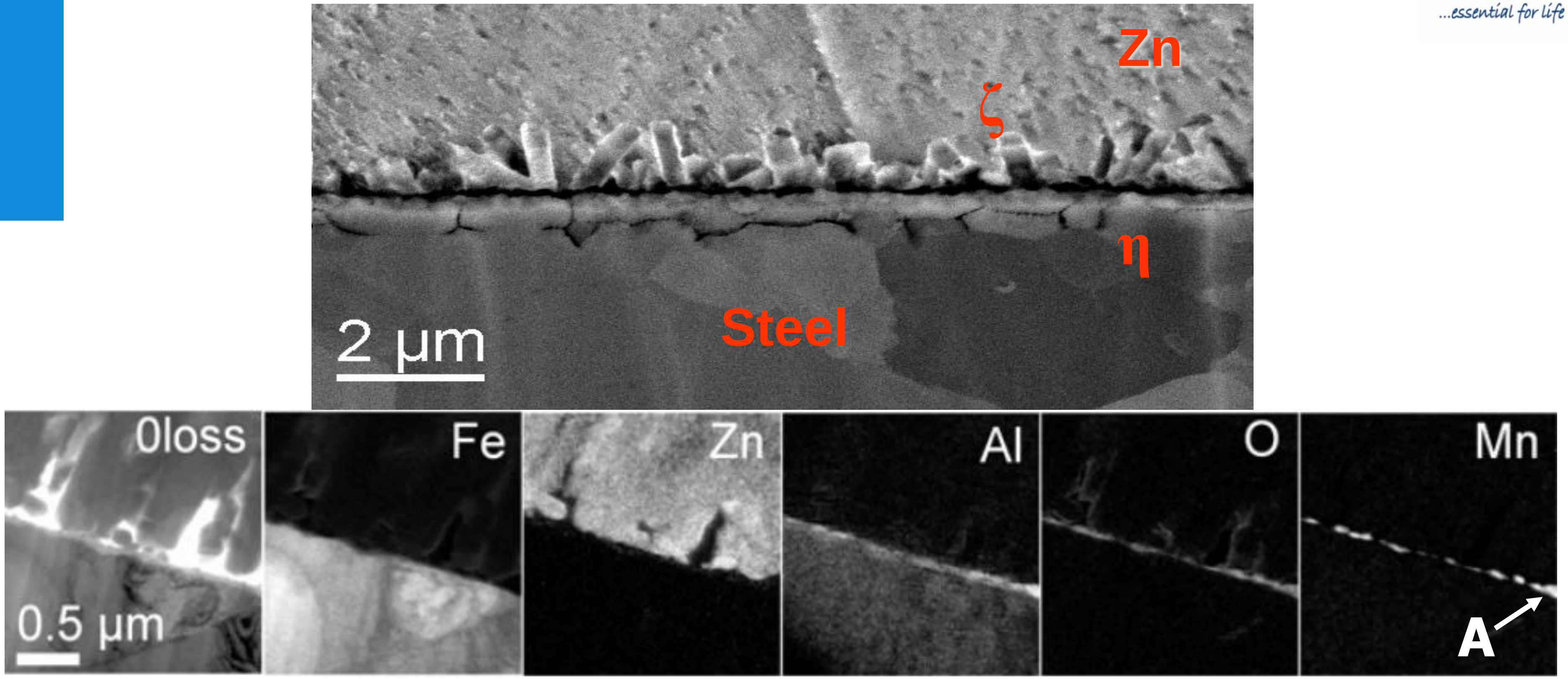

A continuous thin layer with high Al content: $Fe_2Al_{5-x}Zn_x$ inhibition layer
Locally high Mn +O concentrations along the Zinc/Steel interface

G.M. Song, T. Vystavel, N. van der Pers, J.T.M. De Hosson, W.G. Sloof, Relation between microstructure and adhesion of hot dip galvanized zinc coatings on dual phase steel, Acta Mater 60(6-7) (2012) 2973-2981

Surface oxides and coating adhesion

Selective oxidation of alloying elements in AHSS

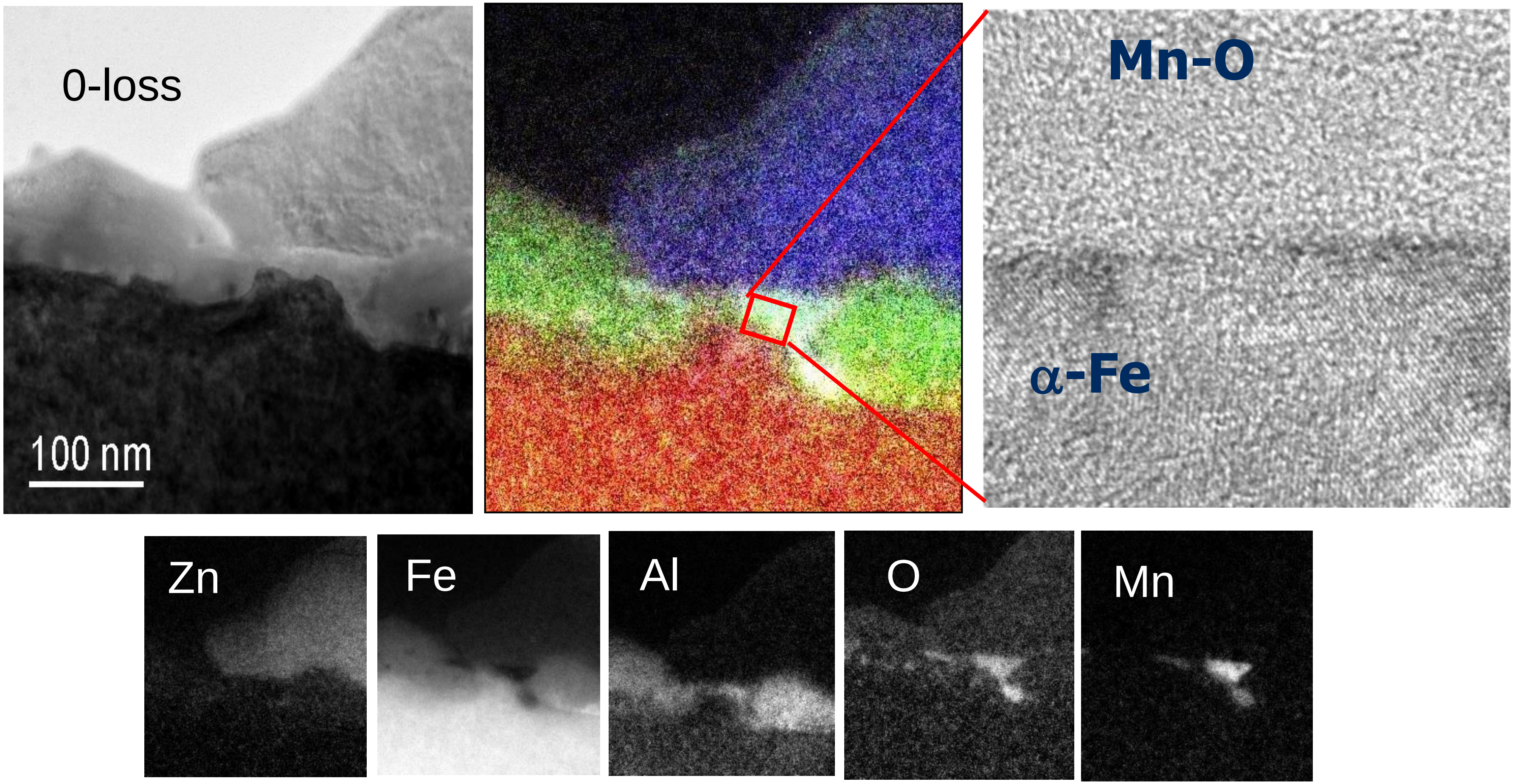

G.M. Song, T. Vystavel, N. van der Pers, J.T.M. De Hosson, W.G. Sloof, Relation between microstructure and adhesion of hot dip galvanized zinc coatings on dual phase steel, Acta Mater 60 (2012) 2973-2981

Effect of surface oxides on Work of Adhesion

Schematic of zinc coating / steel interface

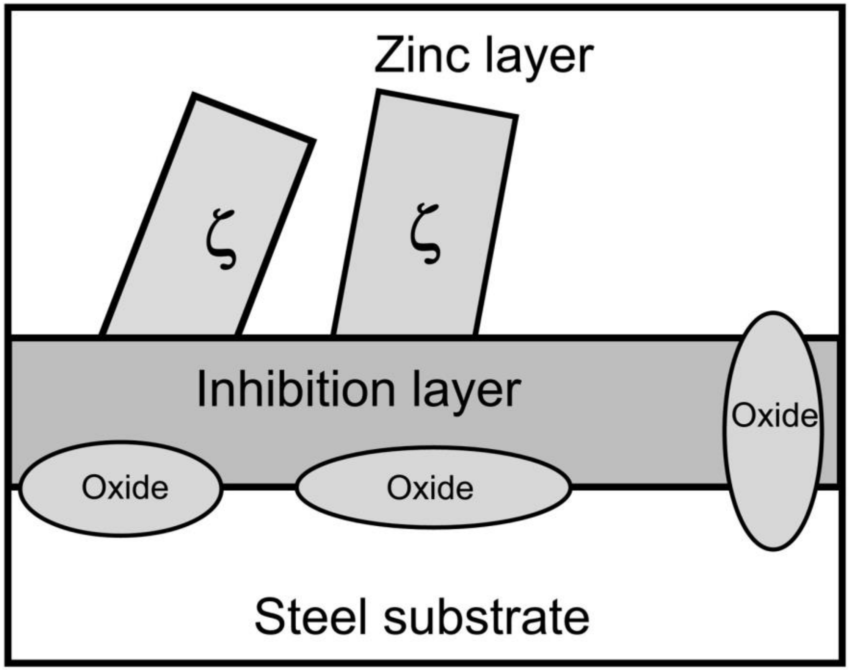

$$W_{Ad} = g^{Met}_{Surface} + g^{Oxide}_{Surface} - g^{Met-Oxide}_{Interface}$$

Interface	W_{Ad}, J/m^2
Steel/Inhibition layer	3.95
Steel/zinc layer	3.24
Inhibition layer/zinc layer	2.90
Al_2O_3/inhibition layer	3.15
Al_2O_3/steel	3.44
Al_2O_3/zinc layer	**2.28**
MnO/inhibition layer	3.07
MnO/steel	3.40
MnO/zinc layer	**2.22**
SiO_2/inhibition layer	2.80
SiO_2/steel	3.07
SiO_2/zinc layer	**1.93**

Gui-Ming Song and Willem G. Sloof: *Effect of alloying element segregation on the work of Ahesion of metallic coating on metallic substrate: application to zinc coatings on steel substrate*, Surface & Coating Technology, 205 (2011) 4632-4639

3.

Annealing experiments

Steel compositions and annealing

Steel compositions (wt%):

C	Mn	Si	Al
0.010	1.8	0.05	0.02
0.104	1.9	0.94	0.017

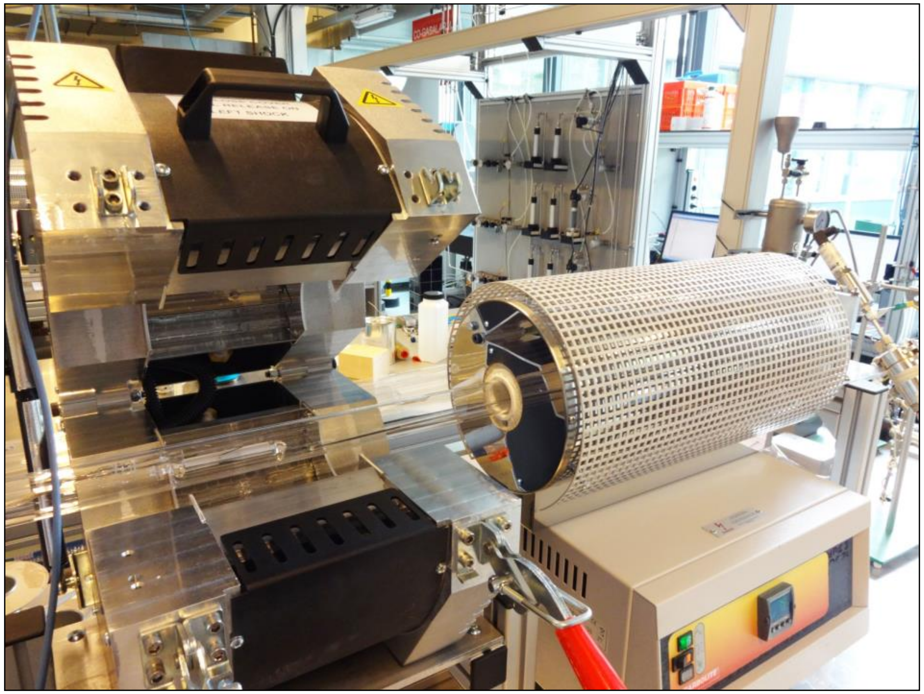

Annealing in Ar + 5 vol. % H_2 with DP's from -70 to +10 ^{o}C @ 950 ^{o}C for 1 h

Using de-ionized water with resistivity of 18.2 MΩ.cm at 25 ^{o}C and de-aerated with N_2 gas

Surface after annealing 1.8 wt% Mn steel

DP -70°C

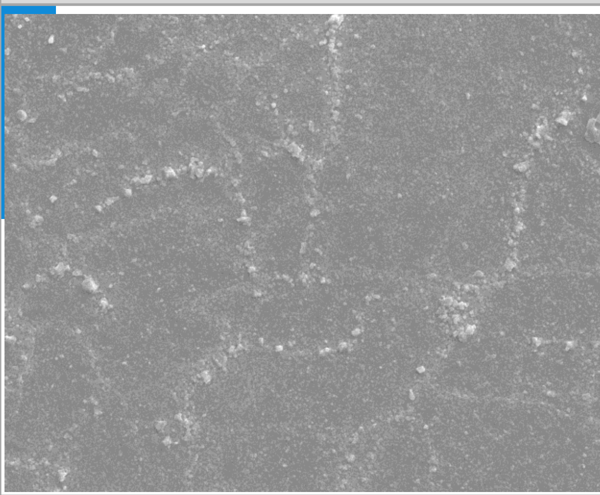

DP -40°C

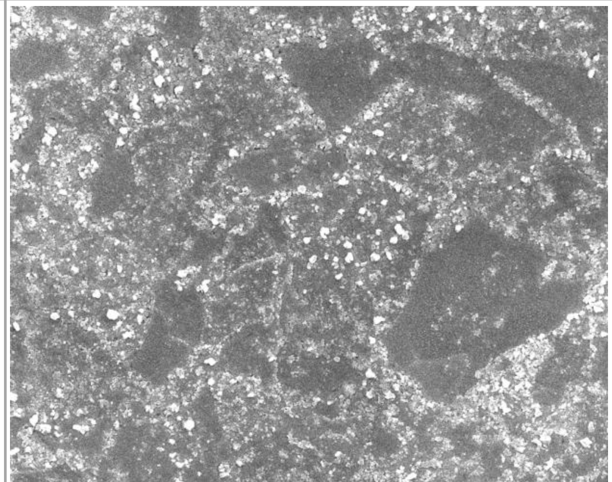

DP -30°C

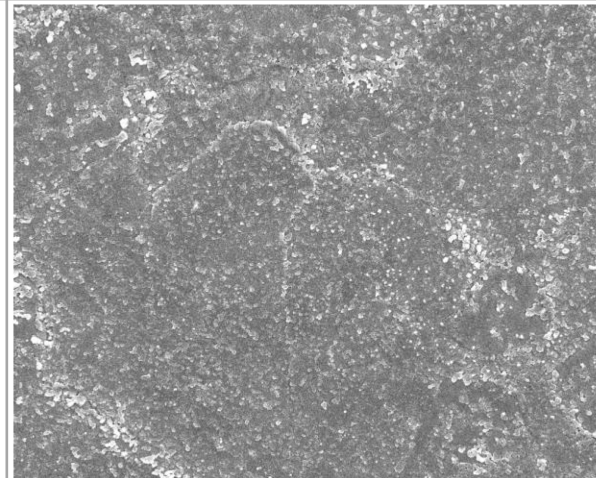

DP 0°C

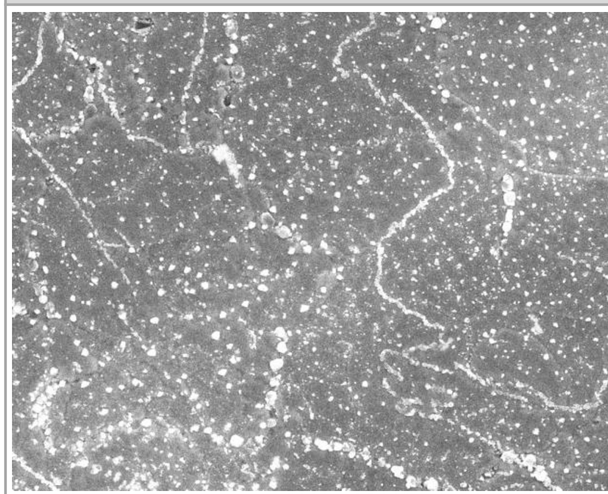

DP +10°C

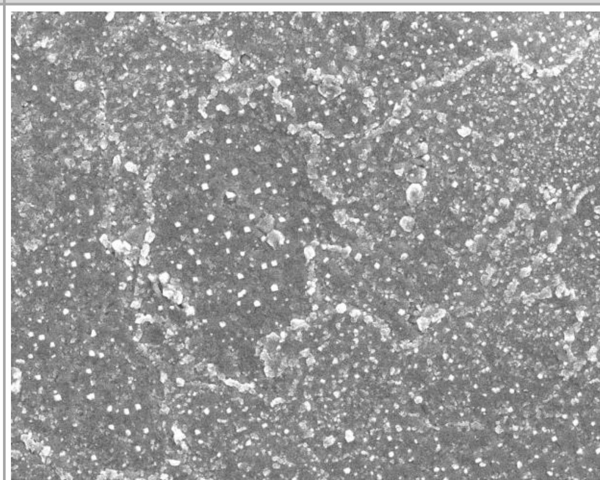

MnO oxides decorating the grain boundaries

SEM 2000x

Surface after annealing 1.9 wt% Mn and 1.0 Si wt% steel

DP -70°C	DP -40°C	DP -30°C
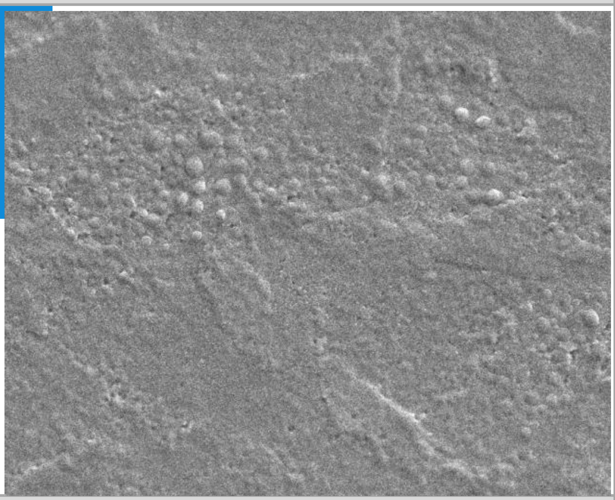	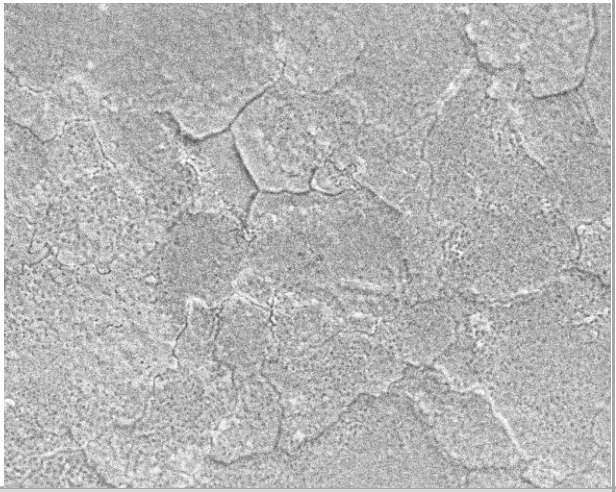	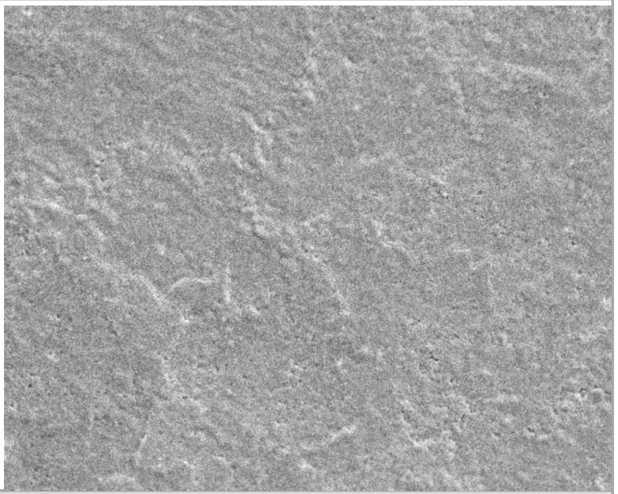
DP 0°C	**DP +10°C**	
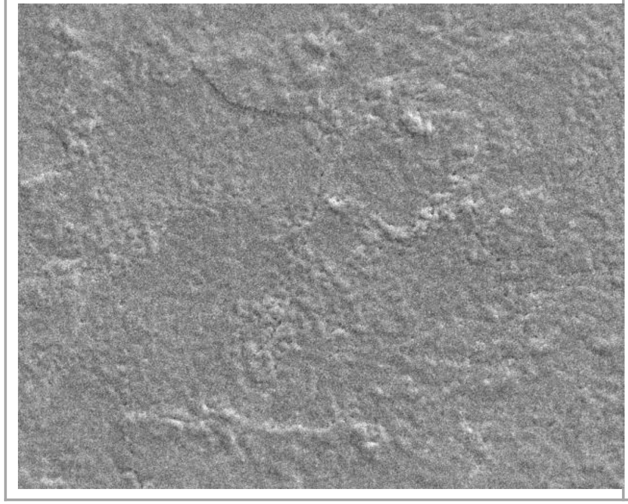	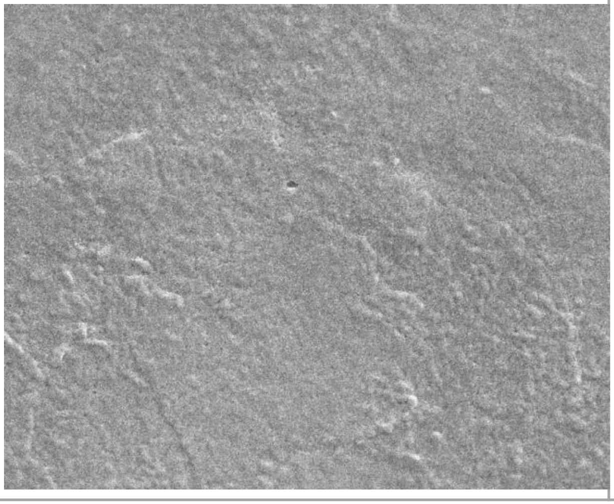	Mn_2SiO_4 oxides covering the surface SEM 2000x

4.

Dewetting experiments

Dewetting Experiments

Pb deposition on steel substrates

500-nm-thick Pb film

Pb film

Steel substrate

Dewetting Pb film into Pb droplets

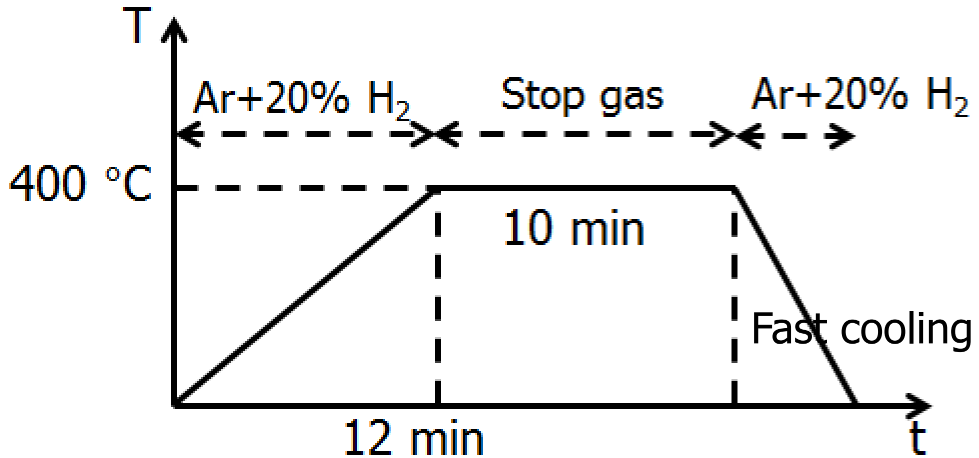

Melting point of Pb: 327.5 °C

Pb droplets

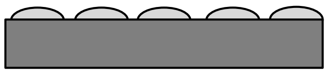

Steel substrate

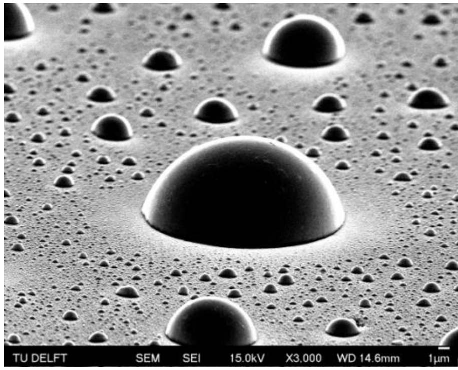

Note: Pb was used because it doesn't react with steels

SEM graphs of Pb particles on steels

Samples tilted 70 °

Pb particles on 1.8 wt% Mn alloyed

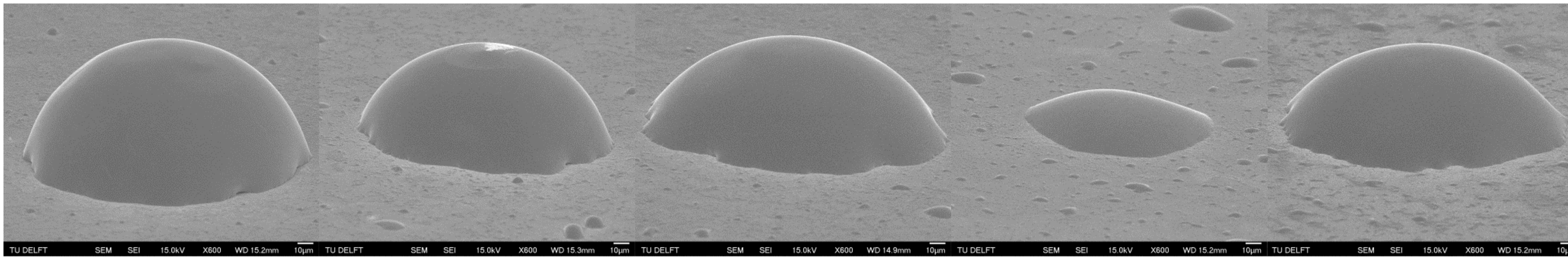

Pb particles on 1.9 wt% Mn-1.0 wt% Si alloyed steel

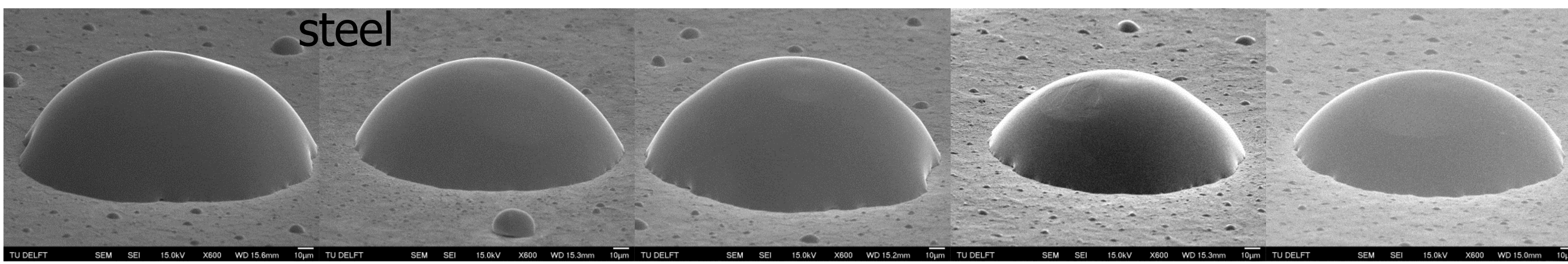

DP: -70 °C -40 °C -30 °C 0 °C 10 °C

Contact angle measurements

Droplets contour line acquisition

SEM graph of tilted sample

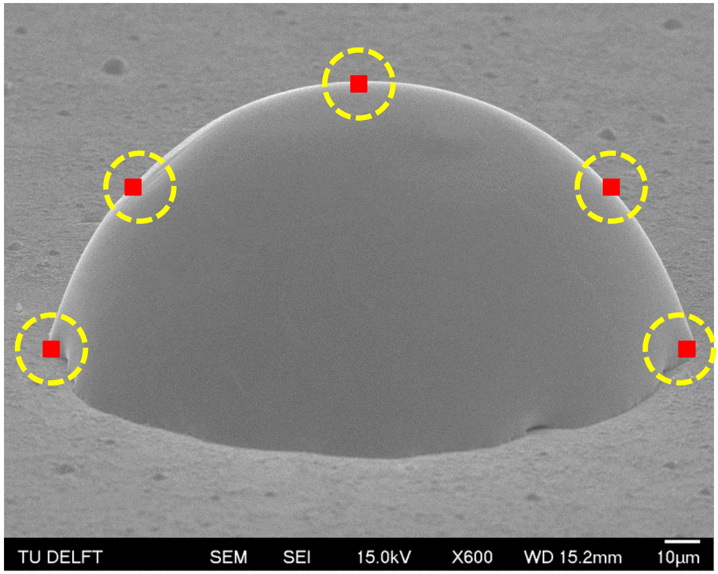

Or

3D graph by Keyence

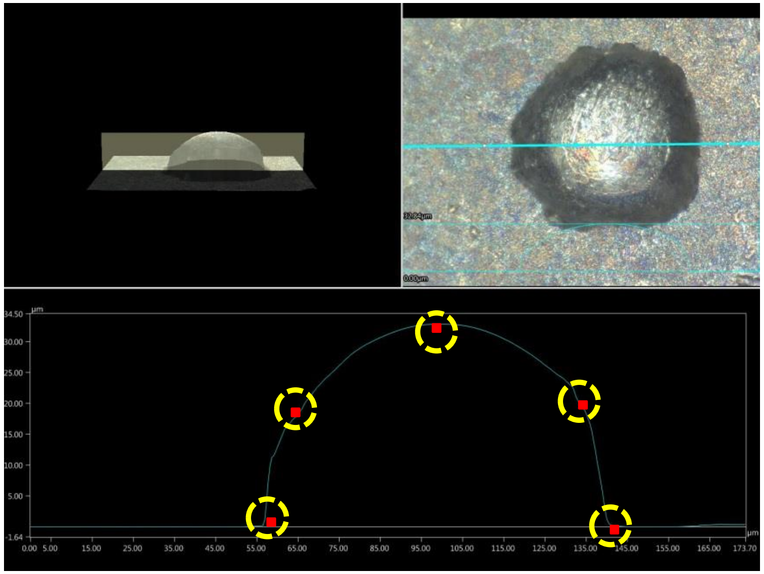

Image J: contact angle plug-in

5 points: 2 at the left and right contact angles, 3 on the drop boundary

Contact angle measurements

Image J: contact angle plug-in

Circle or ellipse fit

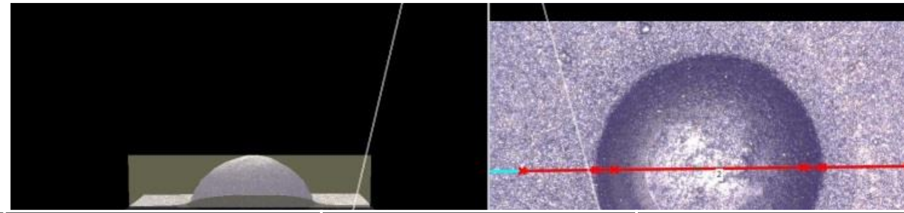

Dew point	-70 ° C	-40 ° C	-30 ° C	-10 ° C	10 ° C
Sample No.	C1	C2	C3	C4	C5
#1	75.7 °	58.3 °	45.8 °	31.7 °	49.9 °
#2	61.2 °	68.0 °	57.2 °	33.4 °	45.7 °
#3	63.9 °	62.5 °	53.8 °	34.0 °	45.6 °
Average	66.9 ° ±7.7 °	62.9 ° ±4.9 °	52.3 ° ±5.9 °	33.0 ° ±1.2 °	47.1 ° ±2.5 °
Sample No.	H1	H2	H3	H4	H5
#1	56.3 °	78.8 °	73.3 °	46.0 °	52.3 °
#2	62.9 °	71.0 °	70.4 °	46.7 °	52.4 °
#3	65.0 °	68.9 °	63.4 °	44.7 °	57.6 °
Average	61.4 ° ±4.5 °	72.9 ° ±5.2 °	69.1 ° ±5.0 °	45.8 ° ±1.0 °	54.1 ° ±3.0 °

Contact angle dew point during annealing

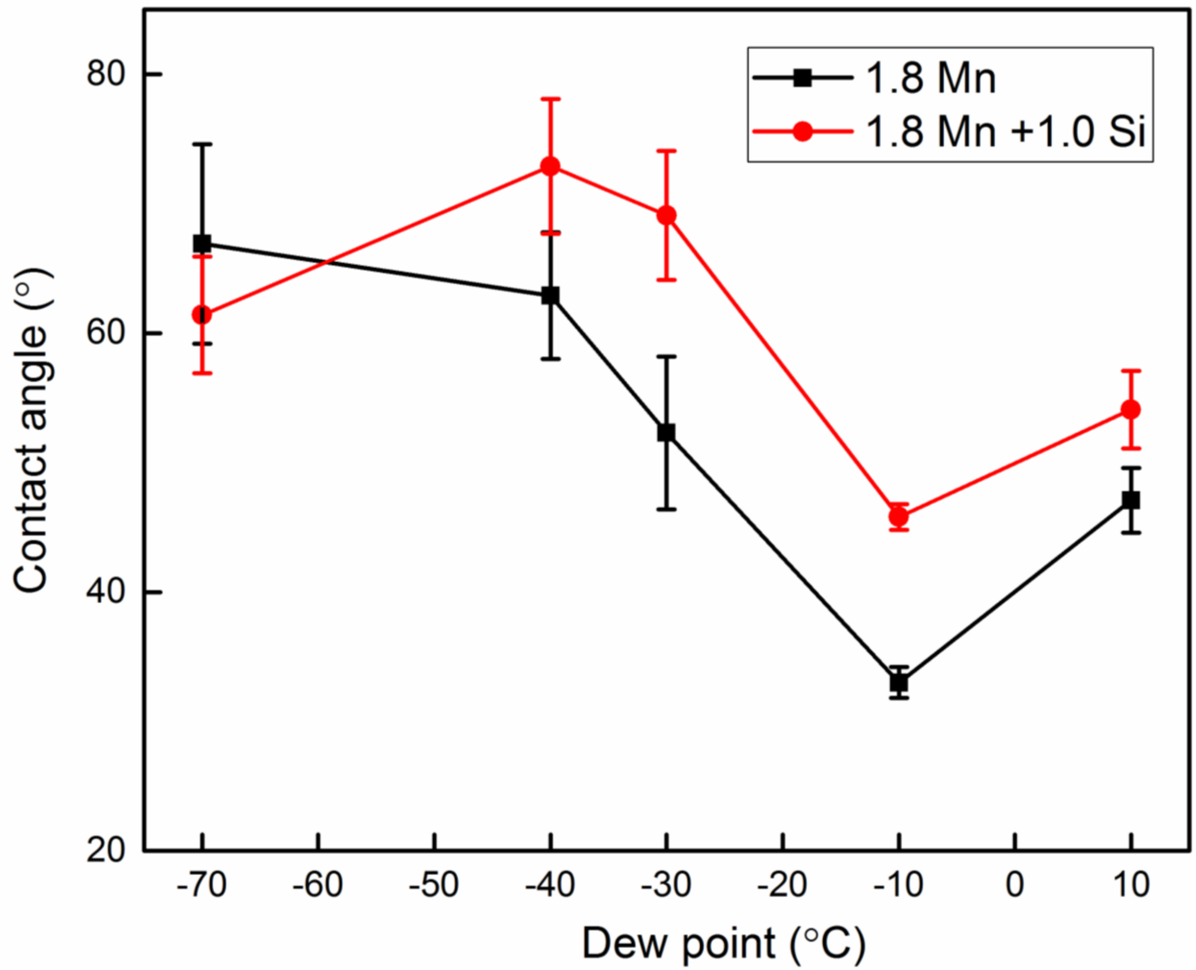

The results suggest that the contact angle decreases with increasing dew point

The improved wetting with increasing dew point may be related to internal oxidation rather than external oxidation

This investigated with XPS analysis of the steel surface after annealing

Surface composition by XPS

Annealing of 1.8 wt% Mn steel in Ar + 5 vol.% H_2 and DP of +10 ^oC

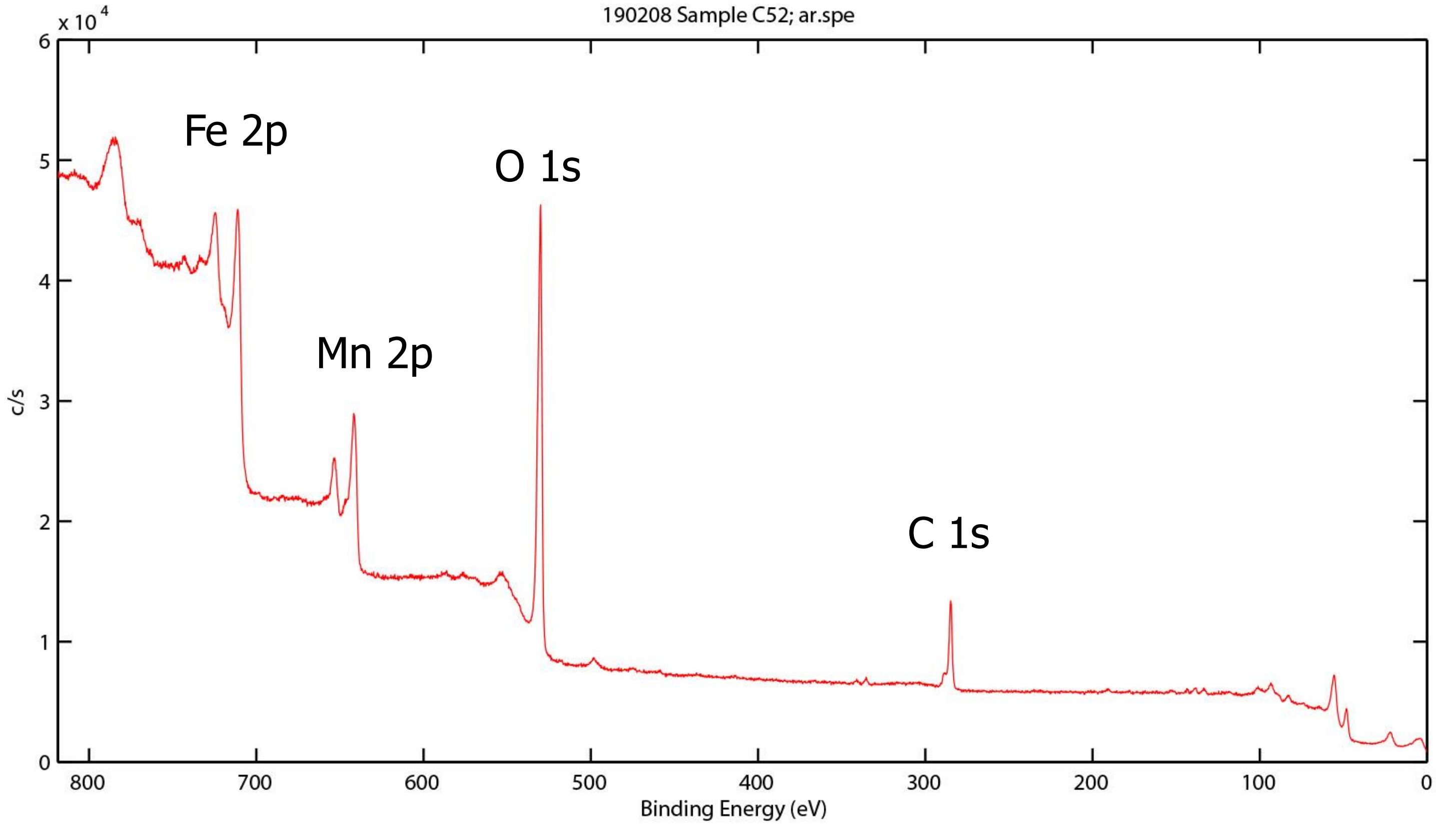

Oxides composed of (Mn,Fe)O where the fraction of Fe depends on DP

Surface composition by XPS

Annealing of 1.9 wt%Mn + 1.0 wt% Si steel in Ar + 5 vol.% H_2 and DP of +10 ^oC

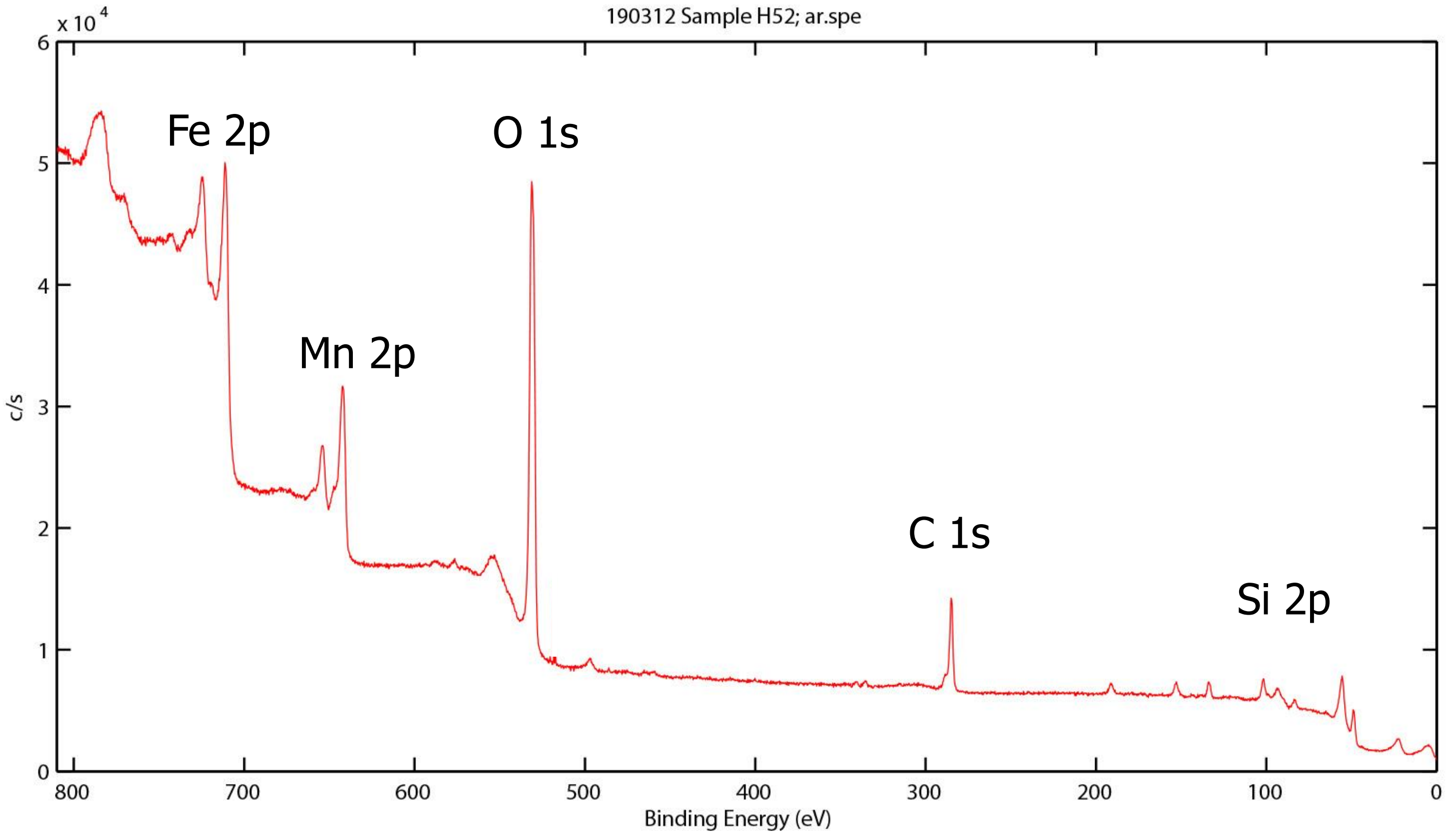

Oxides composed of $(Mn,Fe)_2SiO_4$ where the fraction Fe depends on DP

Surface composition by XPS

Annealing of 1.9 wt%Mn + 1.0 wt% Si steel in Ar + 5 vol.% H_2

Blue DP of +10 ^{o}C and Red DP of -40 ^{o}C

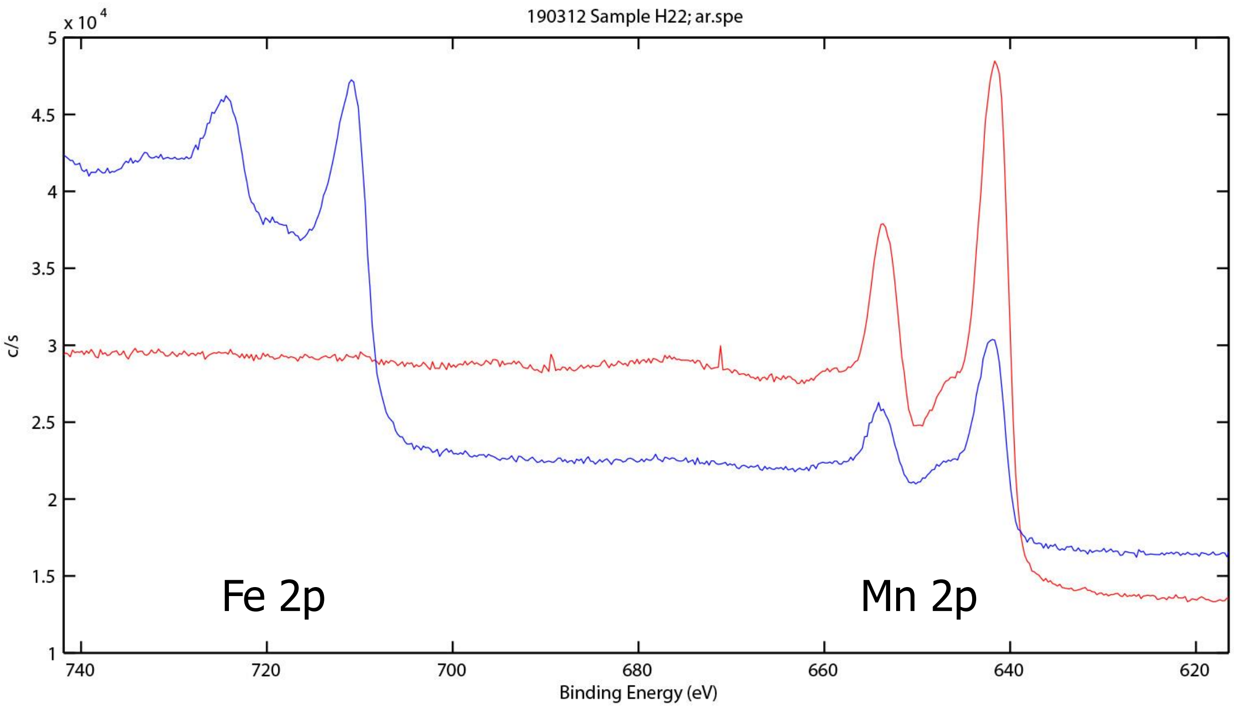

Note that no Fe 2p signal of the steel substrate is observed after annealing at low DP

Low DP surface entirely covered with oxide Mn_2SiO_4

High DP oxides composed of $(Mn,Fe)_2SiO_4$

Contact angle vs surface composition

Annealing of 1.9 wt%Mn + 1.0 wt% Si steel in Ar + 5 vol.% H_2

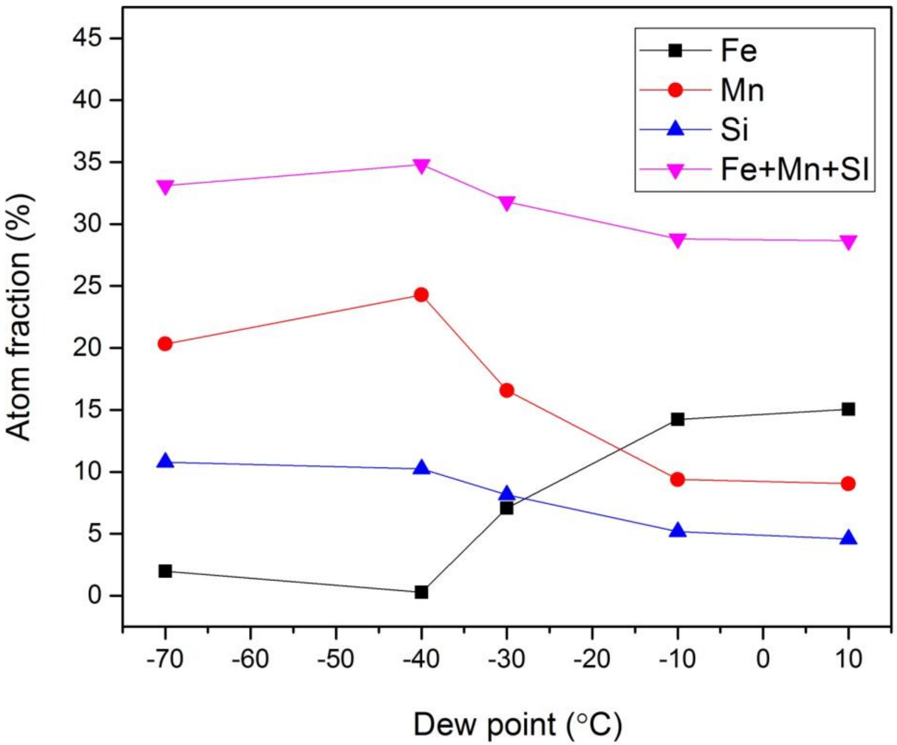

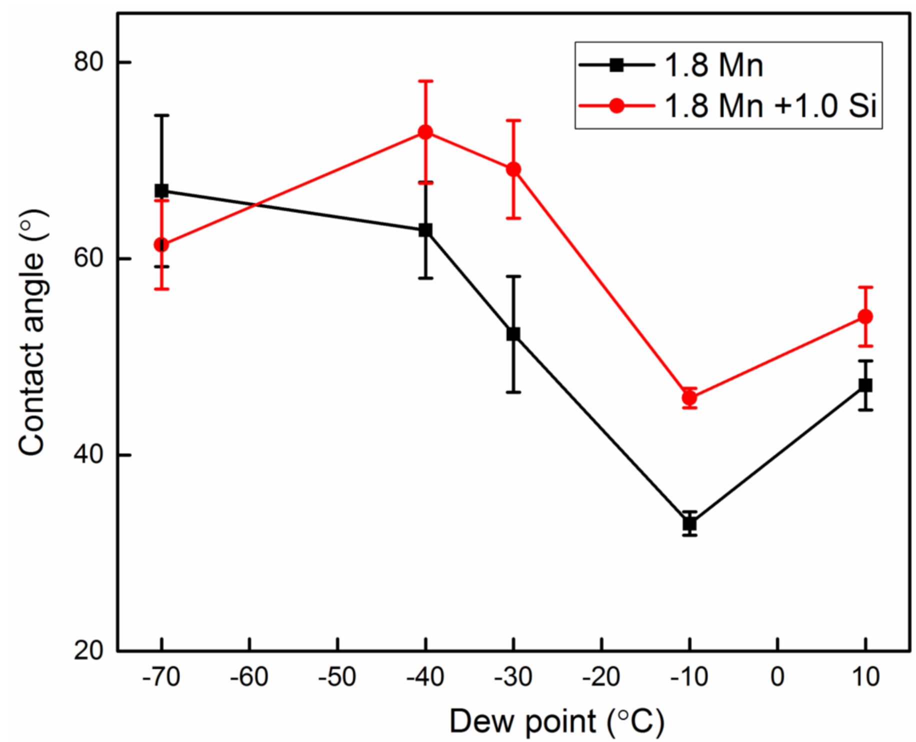

Oxides composed of $(Mn,Fe)_2SiO_4$ where the fraction Fe depends on DP

Composition of the oxides at the surface show a similar trend as the contact angle

5.

Contact Angle and Work of Adhesion

Relationship between contact angle and Work of Adhesion

Young's equation:

$$\cos\theta_Y = \frac{\gamma_{sv} - \gamma_{sl}}{\gamma_{lv}}$$

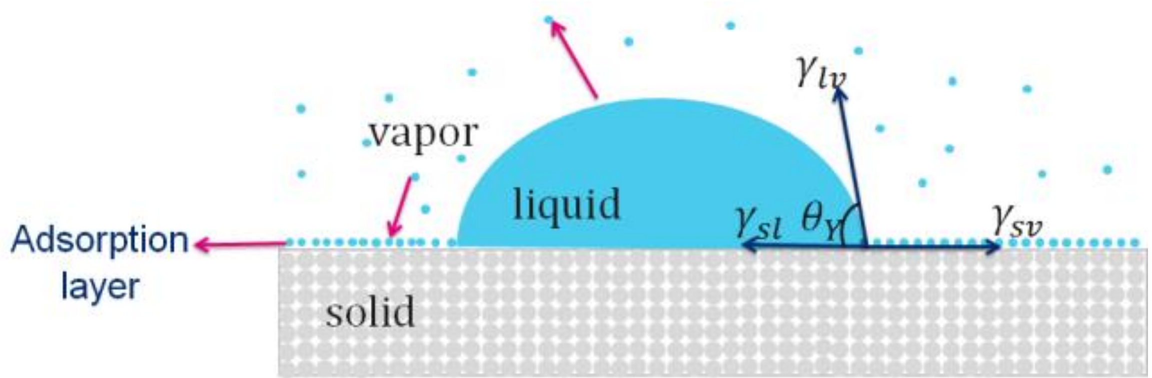

Work of Adhesion (*WoA*):

$$WoA = \gamma_{lv} + \gamma_{sv} - \gamma_{sl}$$

Young-Dupré equation:

$$WoA = \left(1 + \cos\theta_Y\right)\gamma_{lv}$$

Estimation of Work of Adhesion from contact angle measurement

Applying to solid-solid interaction:

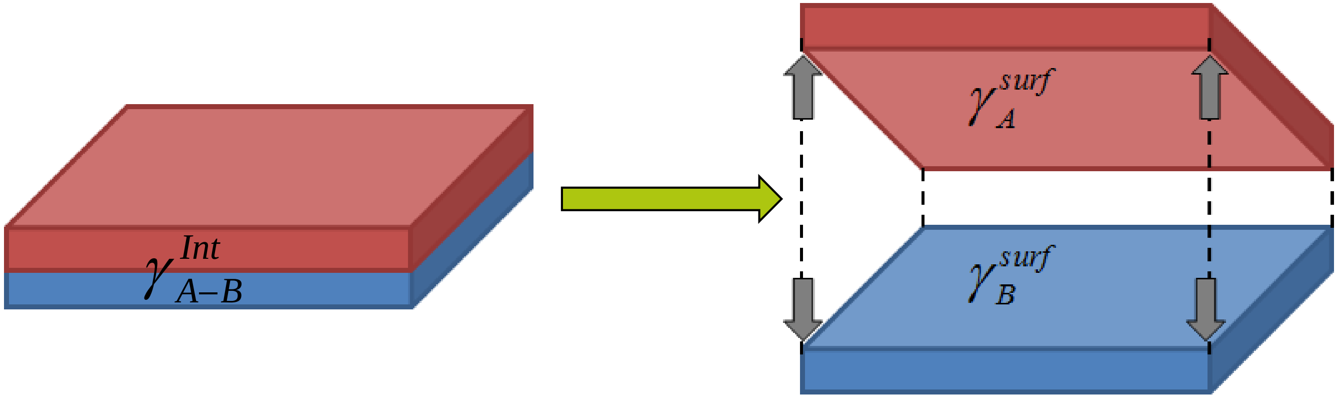

$$WoA = \gamma_{A}^{surf} + \gamma_{B}^{surf} - \gamma_{A-B}^{Int} = (1+\cos\theta_{A-B})\gamma_{A}^{surf}$$

$$\theta_{A-B} : contact\ angel\ of\ solid\ A\ on\ solid\ B$$

$$How\ to\ obtain\ \theta_{A-B}\ ?$$

Estimation of Work of Adhesion from contact angle measurement

Annealing for 24 h after dewetting

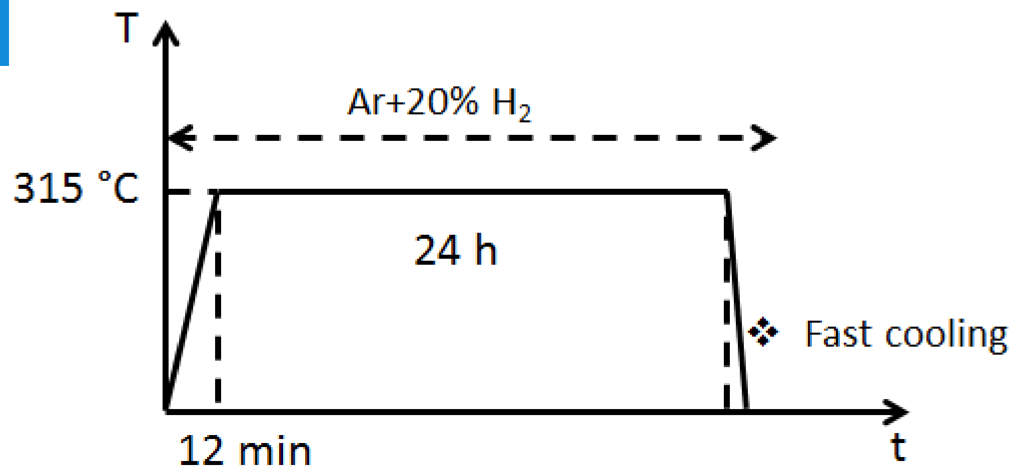

❖ Melting point of Pb: 327.5 °C

Pb/Fe	Before annealing	After annealing
Contact angle	68.5°±5.2°	68.6°±4.8°

Contact angles don't change much before and after annealing.

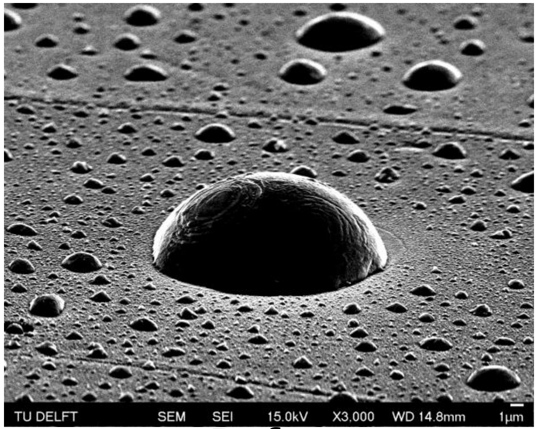

Before

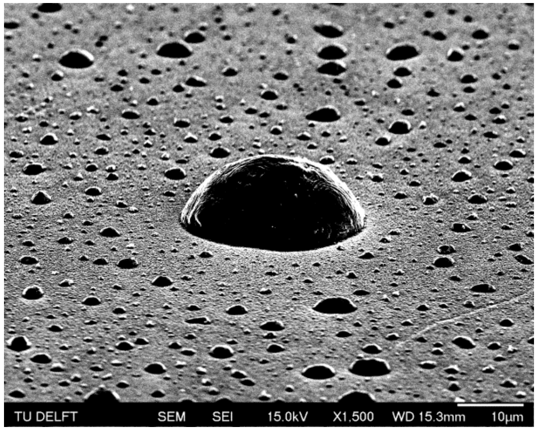

After

Prediction of Work of Adhesion from thermodynamic model

$$WoA = \gamma_A^{surf} + \gamma_B^{surf} - \gamma_{A-B}^{Int} = (1+\cos\theta_{A-B})\gamma_A^{surf}$$

$$\gamma_B^o = \frac{\Delta H_B^{vap}}{c_0 V_B^{2/3}} \qquad \gamma_B^{surf} = \gamma_B^o - \pi$$

Spreading pressure

$$\gamma_{A-B}^{Int} = \frac{\Delta H_B^{fuse}}{c_0 V_B^{2/3}} + \frac{2RT}{c_0 V_A^{2/3}} + \frac{\Delta \bar{H}_{B\,in\,A}^{\circ interface}}{c_0 V_B^{2/3}}$$

Spreading pressure: effect of adsorption on surface energy

F.R.de Boer, R. Boom, W.C.M. Mattens, A.R. Miedema, and A.K. Niessen, in Cohesion in Metals: Transition Metals Alloys (North-Holland, Amsterdam, 1988)

Spreading pressure

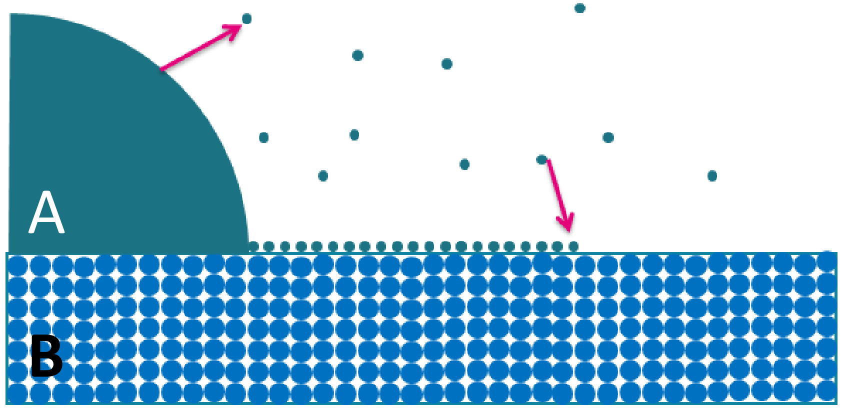

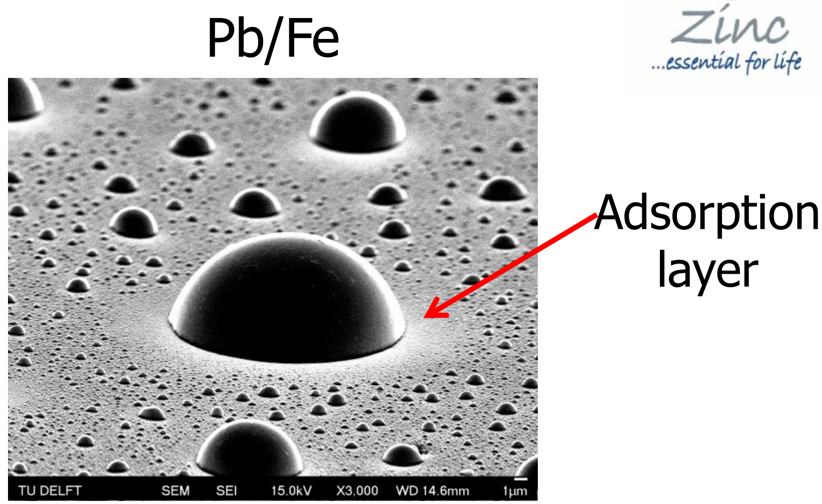

Gibbs adsorption equation: $\left(\frac{\partial \gamma}{\partial \mu}\right)_T = -\Gamma$ adsorption isotherm

$$\pi = -\int_{\mu_A}^{\mu_A'} \Gamma_A d\mu_A = -\frac{RTv^A}{N}\sum_i \ln(1-Y_i^A)$$

v^A: number of atoms per unit area on an A surface
N: Avogadro's number
Y_i^A: coverage of atoms A in each near-surface atomic layer, i

6.

Summary and Future Work

Summary

- Internal rather than external oxidation during annealing of Mn alloyed steels is promoted with increasing dew point
- Addition of Si enhances external oxidation and formation of oxides along grain boundaries
- The contact angle of Pb on the steel surfaces after annealing decreases with increasing dew point; this correlates with increasing amount of Fe in the oxides
- The work of adhesion of coatings on steels can be estimated from contact angle measurements
- The work of adhesion can be predicted by calculating surface and interface energies from a thermodynamic model

Future work

- Determine spreading pressure form AES measurements
- Prediction of contact angle using thermodynamic model
- Look into the effect of surface segregation of alloying elements like Mn and Si on oxidation and coating adhesion

Fe-Mn alloys

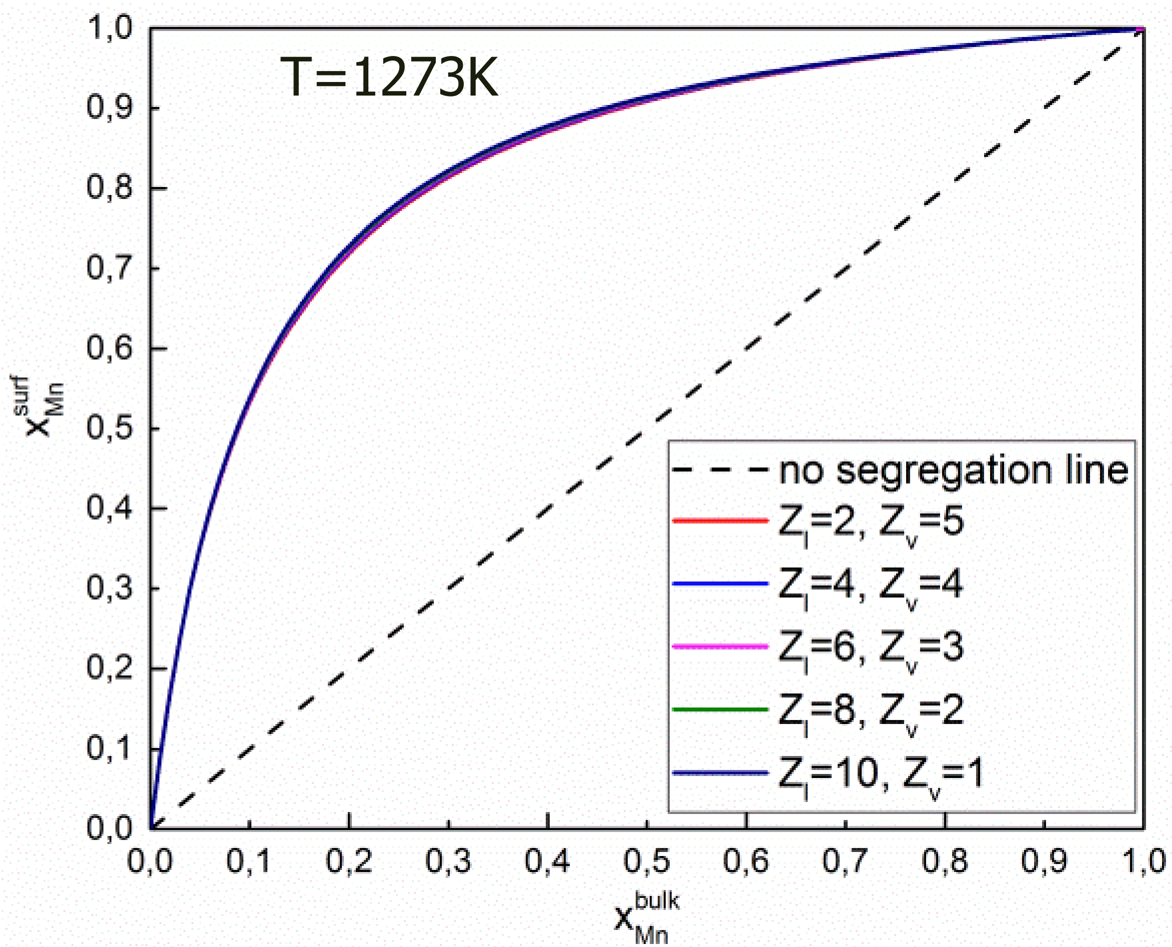

$$Z = Z_l + 2Z_v = 12$$

Strong segregation of Mn to the surface

Fe-Si alloys

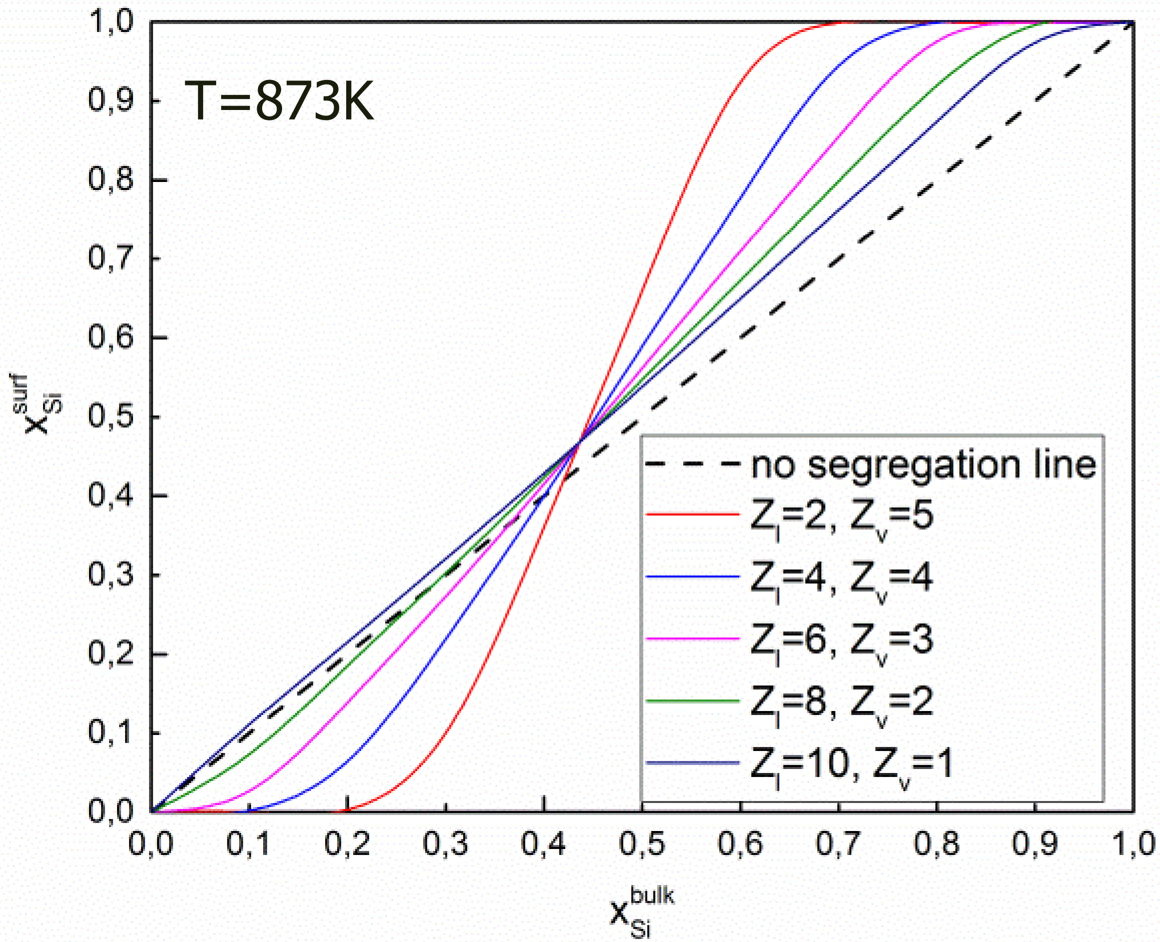

Segregation of Fe to the surface